Fourier transform infrared emission spectra of MgH and MgD

A. Shayesteh and D. R. T. Appadoo
Department of Chemistry, University of Waterloo, Waterloo, Ontario, N2L 3G1, Canada

I. Gordon
Department of Physics, University of Waterloo, Waterloo, Ontario, N2L 3G1, Canada

R. J. Le Roy
Guelph-Waterloo Centre for Graduate Work in Chemistry and Biochemistry, University of Waterloo, Waterloo, Ontario, N2L 3G1, Canada

P. F. Bernath[a)]
Department of Chemistry and Department of Physics, University of Waterloo, Waterloo, Ontario, N2L 3G1, Canada

(Received 9 February 2004; accepted 8 March 2004)

High resolution Fourier transform infrared emission spectra of MgH and MgD have been recorded. The molecules were generated in an emission source that combines an electrical discharge with a high temperature furnace. Several vibration–rotation bands were observed for all six isotopomers in the $X\,^2\Sigma^+$ ground electronic state: $v=1\rightarrow0$ to $4\rightarrow3$ for ^{24}MgH, $v=1\rightarrow0$ to $3\rightarrow2$ for ^{25}MgH and ^{26}MgH, $v=1\rightarrow0$ to $5\rightarrow4$ for ^{24}MgD, $v=1\rightarrow0$ to $4\rightarrow3$ for ^{25}MgD and ^{26}MgD. The new data were combined with the previous ground state data, obtained from diode laser vibration–rotation measurements and pure rotation spectra, and spectroscopic constants were determined for the $v=0$ to 4 levels of ^{24}MgH and the $v=0$ to 5 levels of ^{24}MgD. In addition, Dunham constants and Born–Oppenheimer breakdown correction parameters were obtained in a combined fit of the six isotopomers. The equilibrium vibrational constants (ω_e) for ^{24}MgH and ^{24}MgD were found to be 1492.776(7) cm^{-1} and 1077.298(5) cm^{-1}, respectively, while the equilibrium rotational constants (B_e) are 5.825 523(8) cm^{-1} and 3.034 344(4) cm^{-1}. The associated equilibrium bond distances (r_e) were determined to be 1.729 721(1) Å for ^{24}MgH and 1.729 157(1) Å for ^{24}MgD. © *2004 American Institute of Physics.* [DOI: 10.1063/1.1724821]

INTRODUCTION

The first laboratory spectrum of magnesium monohydride was studied in 1926 when Watson and Rudnick[1] attempted to identify strong bands appearing in astronomical spectra. MgH has become an important molecule in astrophysics, and lines of the $A\,^2\Pi-X\,^2\Sigma^+$ transition (green bands) appear strongly in the absorption spectra of the sun[2] and of late-type stars.[3] Magnesium has three stable isotopes, ^{24}Mg, ^{25}Mg, and ^{26}Mg, with terrestrial abundances[4] 78.99:10.00:11.01, but with different ratios in different stars.[5] Lines of the $B'\,^2\Sigma^+-X\,^2\Sigma^+$ transition of MgH have been found in the spectra of sunspot umbrae,[6] and are useful for the determination of magnesium isotopic abundances. Due to its importance in astrophysics, the line and continuum opacities of MgH in cool stellar atmospheres have been recently calculated.[7,8]

The visible spectra of MgH and MgD have been studied extensively by Balfour and co-workers[9–15] in 1970s. They used a magnesium dc arc in hydrogen or deuterium to generate the molecules, and recorded the $A\,^2\Pi\rightarrow X\,^2\Sigma^+$ and the $B'\,^2\Sigma^+\rightarrow X\,^2\Sigma^+$ transitions of all six isotopomers, i.e., ^{24}MgH, ^{25}MgH, ^{26}MgH, ^{24}MgD, ^{25}MgD, and ^{26}MgD, with a classical spectrograph. This comprehensive analysis led to an experimental value of 1.27(3) eV for the dissociation energy of the $X\,^2\Sigma^+$ ground state of MgH.[15] Parallel to the experimental work in 1970s, several *ab initio* calculations were performed for the ground state and the low-lying excited states.[16–21] A nearly complete set of laboratory references to work prior to 1977 was compiled by Huber and Herzberg.[22]

Bernath *et al.* recorded the emission spectrum of the $A\,^2\Pi\rightarrow X\,^2\Sigma^+$ transition of MgH using a magnesium hollow cathode discharge and a Fourier transform spectrometer.[23] They predicted highly accurate vibration–rotation and pure rotational transition frequencies for the $X\,^2\Sigma^+$ ground electronic state. The pure rotational transitions of ^{24}MgH and ^{24}MgD were then identified in the far infrared spectral region.[24–26] High resolution infrared spectra of MgH and MgD were obtained by Lemoine *et al.*[27] using a diode laser infrared spectrometer, and lines from two vibration-rotation bands, $v=1\leftarrow0$ and $v=2\leftarrow1$, were identified. A few years later, some pure rotational lines of ^{24}MgH, ^{26}MgH, and ^{24}MgD were measured with very high accuracy in the millimeter-wave region.[28]

We report here the high resolution Fourier transform infrared emission spectra of MgH and MgD, containing vibration–rotation bands in the $X\,^2\Sigma^+$ ground electronic state for all six isotopomers. The new infrared spectra have substantially extended the available high resolution ground state data, and have thus led to improved molecular con-

a)Author to whom all correspondence should be addressed. Electronic mail: bernath@uwaterloo.ca

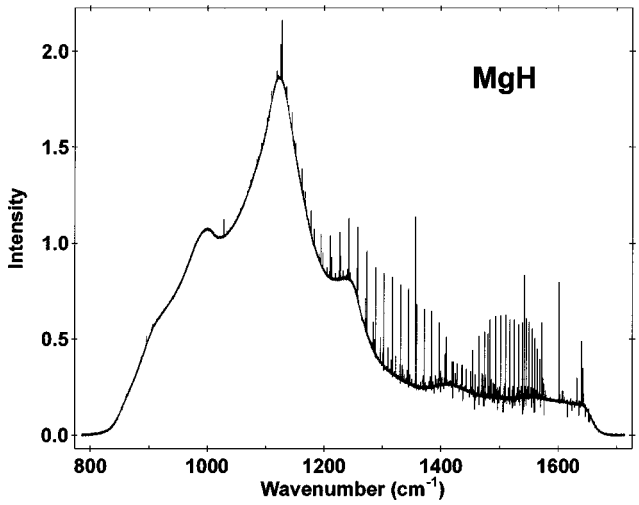

FIG. 1. An overview of the infrared emission spectrum of MgH. The absorption lines are from atmospheric water vapor.

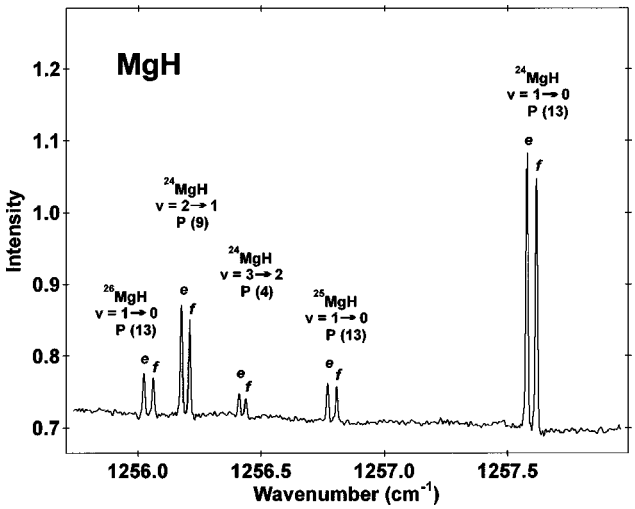

FIG. 3. An expanded view of the MgH spectrum showing the spin splitting in P-branch lines.

stants. We also report a study of the breakdown of the Born–Oppenheimer approximation, which consisted of a combined isotopomer analysis of all the vibration–rotation and pure rotation data for the six species.

EXPERIMENTAL DETAILS

The high resolution emission spectra of MgH and MgD were recorded with a Fourier transform spectrometer in the course of our work on MgH_2 and MgD_2.[29,30] MgH and MgD were generated in an emission source that combines an electrical discharge with a high temperature furnace. About 20–50 grams of magnesium metal was placed inside the central part of an alumina tube (120 cm long and 5 cm in diameter), and heated to 550 °C–650 °C by a CM Rapid Temp furnace. Two stainless steel tube electrodes were placed inside the water-cooled ends of the alumina tube, which were sealed by BaF_2 or CaF_2 windows. A mixture of argon and hydrogen or deuterium with a total pressure of 1–2.5 Torr flowed through the cell, and a dc discharge (3 kV, 333 mA) was applied between the stainless steel electrodes. The emission from the source was focused onto the entrance aperture of a Bruker IFS HR 120 Fourier transform spectrometer, using BaF_2 or CaF_2 lenses.

Several high resolution emission spectra of MgH and MgD were recorded in the 11 000–23 000 cm^{-1} (visible) region using a visible quartz beamsplitter and a silicon photodiode detector. The visible spectra contain many vibrational bands of the $A\,^2\Pi \rightarrow X\,^2\Sigma^+$ and the $B'\,^2\Sigma^+ \rightarrow X\,^2\Sigma^+$ transitions of all six isotopomers. Analysis of the visible spectra is in progress, and will be published separately. In addition, we have recorded and analyzed the infrared spectra of MgH and MgD in the 800–2200 cm^{-1} region, and these results are presented in this paper.

The first MgH infrared spectrum was recorded at 650 °C with 1.6 Torr of argon and 0.9 Torr of hydrogen. A CaF_2 lens and windows were used with a CaF_2 beamsplitter along with a HgCdTe (MCT) detector. The instrumental resolution was 0.01 cm^{-1}, and the spectral region was limited to

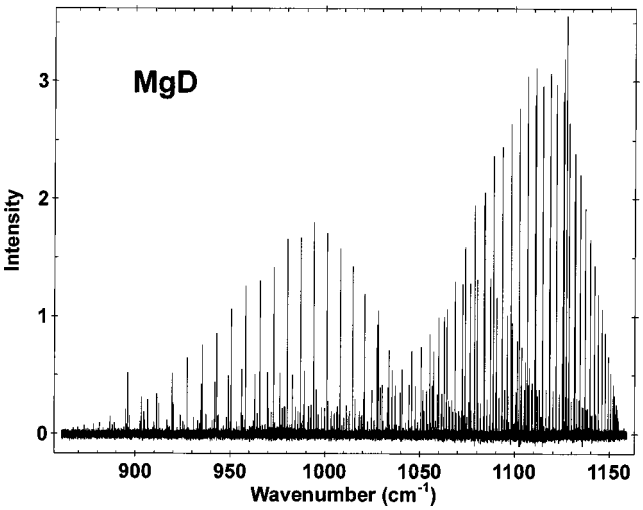

FIG. 2. An overview of the infrared emission spectrum of MgD after baseline correction.

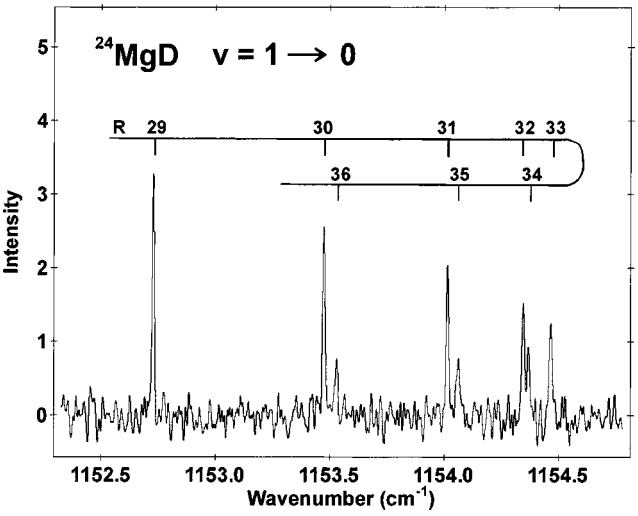

FIG. 4. An expanded view of the R-branch head in the $v=1\rightarrow 0$ band of ^{24}MgD.

TABLE I. Spectroscopic constants (in cm^{-1}) for the $X\ ^2\Sigma^+$ ground state of ^{24}MgH (all uncertainties are 2σ).

v	T_v	B_v	$10^4\ D_v$	$10^9\ H_v$	$10^{12}\ L_v$	$10^2\ \gamma_v$	$10^6\ \gamma_{D,v}$
0	0.0	5.736 5078(4)	3.543 234(130)	14.537(38)	−1.38(3)	2.638 97(11)	−5.77(10)
1	1431.977 78(18)	5.555 2881(5)	3.557 26(14)	13.197(35)	−1.81(3)	2.524 80(11)	−5.79(10)
2	2800.6770(4)	5.367 5658(79)	3.601 13(53)	11.07(12)	−2.60(8)	2.401(5)	−5.8(1)
3	4102.3284(5)	5.169 804(15)	3.6895(13)	6.91(38)	−3.6(4)	2.273(8)	−6.0(3)
4	5331.3869(10)	4.956 662(30)	3.8506(22)	−2.8(5)		2.126(20)	−6.0(10)

$1200-2200\ cm^{-1}$ by the CaF_2 beamsplitter and a $2200\ cm^{-1}$ long-wave pass filter. In order to improve the signal-to-noise ratio, about 550 scans were co-added during 8 hours of integration. The second MgH infrared spectrum (550 scans) was recorded at 550 °C with ~1 Torr of pure hydrogen. A BaF_2 lens and windows were used with a KBr beamsplitter and a HgCdTe (MCT) detector. The instrumental resolution was again $0.01\ cm^{-1}$, and the spectral bandpass was set to $800-1700\ cm^{-1}$ by the detector response, the BaF_2 optics, and a $1700\ cm^{-1}$ long-wave pass filter. The infrared spectrum of MgD was recorded at 600 °C with ~1 Torr of pure deuterium. All other conditions were the same as in the second MgH experiment, and in this case 1200 scans were co-added during 18 hours of integration. The spectra contained atomic and molecular emission lines, as well as blackbody emission from the hot tube and absorption lines from atmospheric water vapor. The signal-to-noise ratios were about 180 and 120 for the strongest MgH and MgD lines, respectively.

RESULTS AND ANALYSIS

The infrared spectra of MgH and MgD contained vibration-rotation bands of all six isotopomers. An overview of the second MgH spectrum, recorded with the $1700\ cm^{-1}$ long-wave pass filter, is shown in Fig. 1. The strongest emission lines in the overview spectrum are from the $v=1\rightarrow0$ fundamental band of ^{24}MgH. In addition, three hot bands of ^{24}MgH, i.e., $v=2\rightarrow1$, $3\rightarrow2$ and $4\rightarrow3$, were found and rotationally analyzed. Due to the low natural abundances of ^{25}Mg (10 %) and ^{26}Mg (11 %), only the $v=1\rightarrow0$ to $v=3\rightarrow2$ bands were observed for ^{25}MgH and ^{26}MgH. A few vibration-rotation bands of $^{24}MgH_2$ and impurity CO were observed in the first MgH spectrum, recorded with the $2200\ cm^{-1}$ long-wave pass filter.[29] Five vibration–rotation bands, from $v=1\rightarrow0$ to $v=5\rightarrow4$, were found for ^{24}MgD. For the minor isotopomers ^{25}MgD and ^{26}MgD, only the $v=1\rightarrow0$ to $v=3\rightarrow2$ and a few R-branch lines of $v=4\rightarrow3$ were observed. In addition, a very weak band of $^{24}MgD_2$ was found and analyzed.[30] An overview of the MgD spectrum is shown in Fig. 2. In order to display the bands clearly, the baseline of the MgD spectrum in Fig. 2 was corrected using the Bruker OPUS program.

The ground electronic state of MgH is a $^2\Sigma^+$ state, in which the e (F_1) and f (F_2) spin components are split by the spin–rotation interaction. All P-branch lines were doubled in the MgH and MgD spectra, while the splitting was observed for only some of the R-branch lines. An expanded view of the MgH spectrum in Fig. 3 shows the splitting of the lines corresponding to e and f parity levels. The $v=1\rightarrow0$ band head of ^{24}MgD is shown in Fig. 4.

Line positions in the spectra were determined using WSPECTRA program[31] written by M. Carleer (Université Libre de Bruxelles). Impurity CO lines were used to calibrate the first MgH spectrum ($1200-2200\ cm^{-1}$), and MgH lines were used to transfer the calibration to the second spectrum ($800-1700\ cm^{-1}$). Both MgH spectra were needed for our data analysis: the first spectrum was used for lines above $1450\ cm^{-1}$, while the second spectrum had a higher signal-to-noise ratio below $1450\ cm^{-1}$. The MgD spectrum was calibrated using several atomic lines common to the MgH and MgD spectra. The absolute accuracy of calibrated line positions is better than $0.001\ cm^{-1}$, and an experimental uncertainty of $0.001\ cm^{-1}$ was assigned to strong unblended lines of ^{24}MgH and ^{24}MgD. For very weak bands, i.e., $v=4\rightarrow3$ band of ^{24}MgH, $v=5\rightarrow4$ band of ^{24}MgD, and the lines from minor isotopomers, an uncertainty of $0.002\ cm^{-1}$ was used. Assignment of the bands was facilitated using a color Loomis–Wood program.

The available diode laser infrared spectra[27] contain lines from the $v=1\leftarrow0$ and $v=2\leftarrow1$ bands of MgH and MgD with an experimental uncertainty of $0.002\ cm^{-1}$, and there is no systematic discrepancy between those lines and our calibrated line positions. We included the diode laser infrared lines and all pure rotational lines[24–26,28] in our data set. We removed the hyperfine structure of the pure rotational lines by using the rotational and spin–rotation interaction constants reported in Refs. 26 and 28 to compute the hyperfine-

TABLE II. Spectroscopic constants (in cm^{-1}) for the $X\ ^2\Sigma^+$ ground state of ^{24}MgD (all uncertainties are 2σ).

v	T_v	B_v	$10^4\ D_v$	$10^9\ H_v$	$10^2\ \gamma_v$	$10^6\ \gamma_{D,v}$
0	0.0	3.000 9455(3)	0.961 742(130)	1.989(15)	1.381 73(11)	−1.49(17)
1	1045.8446(3)	2.933 3697(27)	0.962 51(12)	1.787(12)	1.338(4)	−1.46(15)
2	2059.3940(4)	2.864 344(4)	0.966 80(13)	1.532(12)	1.288(8)	−1.2(3)
3	3039.5181(5)	2.793 330(7)	0.976 18(22)	1.23(2)	1.233(9)	
4	3984.7236(8)	2.719 587(13)	0.991 72(50)	0.76(5)	1.19(2)	
5	4893.041(6)	2.642 114(44)	1.0156(8)			

TABLE III. A comparison of ^{24}MgH and ^{24}MgD constants for $v=0$ (all values are in cm^{-1}, and all uncertainties are 2σ).

Molecule		B_0	$10^4\ D_0$	$10^9\ H_0$	$10^{12}\ L_0$	$10^2\ \gamma_0$	$10^6\ \gamma_{D,0}$
^{24}MgH	This work	5.736 5078(4)	3.543 234(130)	14.537(38)	−1.38(3)	2.638 97(11)	−5.77(10)
	Ref. 28	5.736 507 83(15)	3.542 85[a]			2.637 855(40)	
	Ref. 27	5.736 5089(36)	3.544 27(164)	16.0(22)		2.638 85(100)	−5.819(136)
	Ref. 26	5.736 5069(12)	3.542 861(554)	14.01(73)		2.638 85(36)	−5.827(53)
^{24}MgD	This work	3.000 9455(3)	0.961 742(130)	1.989(15)		1.381 73(11)	−1.49(17)
	Ref. 28	3.000 945 74(36)	0.961 965(511)			1.381 753(89)	−1.53(16)
	Ref. 27	3.000 9462(22)	0.962 12(62)	2.25(60)		1.3776(26)	−1.34(34)

[a]Fixed to the value taken from Ref. 26.

free line positions. A complete list of all line positions used in the analysis have been placed in Electronic Physics Auxiliary Publication Service (EPAPS).[32]

A Hamiltonian operator that includes rotation and spin-rotation terms,

$$\hat{\mathbf{H}}=B\hat{\mathbf{N}}^2-D\hat{\mathbf{N}}^4+H\hat{\mathbf{N}}^6+L\hat{\mathbf{N}}^8+\hat{\mathbf{N}}\cdot\hat{\mathbf{S}}(\gamma+\gamma_D\hat{\mathbf{N}}^2), \qquad (1)$$

was used to obtain analytical expressions for the energy levels. The experimental data for $v=0$ to 4 of ^{24}MgH and $v=0$ to 5 of ^{24}MgD were fitted to the analytical energy expressions derived from Eq. (1), using the program DParFit,[33] and the usual band constants of Tables I and II were determined. For more than half of the R-branch lines, the e and f splitting was not observed in our spectra, and for these lines the spin-rotation interaction part of the Hamiltonian, Eq. (1), was set to zero. The $v=5\rightarrow4$ band of ^{24}MgD was very weak, and only 12 unresolved R-branch lines were observed. Therefore, we were unable to determine the spin–rotation interaction constants for the $v=5$ level of ^{24}MgD. To minimize the number of digits required to accurately reproduce the data, the fit to determine the constants of Tables I and II applied the sequential rounding and refitting procedure,[34] starting from the highest order parameter of the highest observed vibrational level.

The new band constants for the $v=0$ levels of ^{24}MgH and ^{24}MgD are compared with the constants previously determined from the diode laser infrared[27] and pure rotational spectra,[26,28] in Table III. Note, however, that we have determined a set of band constants for the $v=0$ to 4 levels of ^{24}MgH and the $v=0$ to 5 levels of ^{24}MgD, while the previous diode laser infrared data included only the $v=0$ to 2 levels.

The spectral line positions of all six isotopomers were also fitted to a Dunham-type energy level expression. Taking

TABLE IV. Dunham and Born–Oppenheimer breakdown constants (in cm^{-1}) for the $X\ ^2\Sigma^+$ ground state of ^{24}MgH and ^{24}MgD (all uncertainties are 2σ).

Dunham	^{24}MgH	^{24}MgD	Born–Oppenheimer breakdown	
$Y_{1,0}$	1492.776 34(720)	1077.297 606	$\delta^{\mathrm{H}}_{1,0}$	0.8092(87)
$Y_{2,0}$	−29.846 82(800)	−15.521 1147	$\delta^{\mathrm{H}}_{2,0}$	0.058(8)
$10\ Y_{3,0}$	−3.0481(390)	−1.183 86	$10\ \delta^{\mathrm{H}}_{3,0}$	−0.2086(270)
$10^2\ Y_{4,0}$	−1.580(84)	−0.389 659	$10^2\ \delta^{\mathrm{H}}_{4,0}$	0.284(32)
$10^3\ Y_{5,0}$	−4.642(67)	−0.907 448		
$Y_{0,1}$	5.825 5229(82)	3.034 343 576	$\delta^{\mathrm{H}}_{0,1}$	0.007 6044(31)
$10\ Y_{1,1}$	−1.772 981(270)	−0.666 066 03	$10\ \delta^{\mathrm{H}}_{1,1}$	−0.001 17(2)
$10^3\ Y_{2,1}$	−1.229(28)	−0.333 0008		
$10^4\ Y_{3,1}$	−4.8579(1200)	−0.949 654		
$10^5\ Y_{4,1}$	3.70(24)	0.521 845		
$10^6\ Y_{5,1}$	−9.232(180)	−0.939 419		
$10^4\ Y_{0,2}$	−3.545 57(34)	−0.962 4685	$10^4\ \delta^{\mathrm{H}}_{0,2}$	−0.0132(2)
$10^6\ Y_{1,2}$	1.140(92)	0.222 855		
$10^6\ Y_{2,2}$	−1.4237(690)	−0.200 798		
$10^7\ Y_{3,2}$	1.80(18)	0.183 162		
$10^8\ Y_{4,2}$	−5.758(160)	−0.422 725		
$10^8\ Y_{0,3}$	1.5126(65)	0.213 336	$\delta^{\mathrm{Mg}}_{1,0}$	−0.018(2)
$10^9\ Y_{1,3}$	−1.253(130)	−0.127 501	$\delta^{\mathrm{Mg}}_{0,1}$	0.000 273(8)
$10^{10}\ Y_{2,3}$	2.10(78)	0.154 172		
$10^{10}\ Y_{3,3}$	−1.507(100)	−0.079 822		
$10^{12}\ Y_{0,4}$	−1.26(4)	−0.0925		
$10^{13}\ Y_{1,4}$	−1.6(7)	−0.084 75		
$10^{13}\ Y_{2,4}$	−1.4(3)	−0.053 501		
$10^2\ \gamma_{0,1}$	2.693 18(33)	1.401 884		
$10^3\ \gamma_{1,1}$	−1.061(9)	−0.398 46		
$10^5\ \gamma_{2,1}$	−4.1(5)	−1.1109		
$10^6\ \gamma_{0,2}$	−5.78(10)	−1.566		

TABLE V. A comparison of equilibrium constants of ^{24}MgH and ^{24}MgD (all uncertainties are 2σ).

	^{24}MgH		^{24}MgD	
Constant	This work	Ref. 27	This work	Ref. 27
$Y_{1,0}$ (cm^{-1})	1492.776(7)	1495.263(4)	1077.298(5)	1078.140(2)
$Y_{2,0}$ (cm^{-1})	−29.847(8)	−31.641(2)	−15.521(4)	−16.1474(5)
$Y_{3,0}$ (cm^{-1})	−0.305(4)		−0.118(1)	
$Y_{4,0}$ (cm^{-1})	−0.0158(8)		−0.0039(2)	
$Y_{5,0}$ (cm^{-1})	−0.004 64(7)		−0.000 91(1)	
B_e (cm^{-1})	5.825 523(8)	5.824 80(3)	3.034 344(4)	3.034 18(1)
r_e (Å)	1.729 721(1)	1.729 828(4)	1.729 157(1)	1.729 204(4)

the spin–rotation interaction into account, additional terms were added to the customary Dunham expansion. The following energy expressions:

$$E^e_{v,N}=\sum_{l,m} Y_{l,m}\left(v+\frac{1}{2}\right)^l[N(N+1)]^m+\frac{1}{2}(N)\times\sum_{l,m}\gamma_{l,m}\left(v+\frac{1}{2}\right)^l[N(N+1)]^{m-1}, \quad (2)$$

$$E^f_{v,N}=\sum_{l,m} Y_{l,m}\left(v+\frac{1}{2}\right)^l[N(N+1)]^m-\frac{1}{2}(N+1)\times\sum_{l,m}\gamma_{l,m}\left(v+\frac{1}{2}\right)^l[N(N+1)]^{m-1} \quad (3)$$

were used for e ($J=N+\frac{1}{2}$) and f ($J=N-\frac{1}{2}$) parities, respectively. In Le Roy's formulation of Born–Oppenheimer breakdown parameters,[35] the Dunham constants of each isotopomer, α, are related to those for a chosen reference isotopomer ($\alpha=1$) by the following equation:

$$Y^{(\alpha)}_{l,m}=\left\{Y^{(1)}_{l,m}+\frac{\Delta M^{(\alpha)}_{\mathrm{Mg}}}{M^{(\alpha)}_{\mathrm{Mg}}}\delta^{\mathrm{Mg}}_{l,m}+\frac{\Delta M^{(\alpha)}_{\mathrm{H}}}{M^{(\alpha)}_{\mathrm{H}}}\delta^{\mathrm{H}}_{l,m}\right\}\left(\frac{\mu_1}{\mu_\alpha}\right)^{m+l/2}. \quad (4)$$

Here, $M^{(\alpha)}_{\mathrm{Mg}}$ and $M^{(\alpha)}_{\mathrm{H}}$ are the masses of the Mg and H atoms in isotopomer α, μ's are the reduced masses, and $\delta^{\mathrm{Mg}}_{l,m}$ and $\delta^{\mathrm{H}}_{l,m}$ are the Born–Oppenheimer breakdown correction parameters for the Mg and H atoms. In the present work ^{24}MgH was chosen as the reference isotopomer ($\alpha=1$). There is also an analogous simple reduced mass scaling relationship between the $\gamma_{l,m}$ constants of different isotopomers:

$$\gamma^{(\alpha)}_{l,m}=\gamma^{(1)}_{l,m}\left(\frac{\mu_1}{\mu_\alpha}\right)^{m+l/2}. \quad (5)$$

The Dunham constants of the reference isotopomer (^{24}MgH) and the Born–Oppenheimer breakdown correction parameters ($\delta^{\mathrm{Mg}}_{l,m}$ and $\delta^{\mathrm{H}}_{l,m}$) were determined in a simultaneous fit to all experimental data for the six isotopomers, using the program DPARFIT;[33] the results are presented in Table IV. The Dunham constants of other isotopomers ($\alpha>1$) are derived from the ^{24}MgH constants and the Born-Oppenheimer breakdown correction parameters using Eqs. (4) and (5). The sequential rounding and refitting technique,[34] starting from the parameter with largest relative uncertainty, has been applied to the constants of Table IV in order to minimize the number of digits required to accurately reproduce the data. The derived Dunham constants for ^{24}MgD in Table IV require more digits, as determined by parameter sensitivities.[34] We do not list the analogous derived Dunham constants of the minor Mg isotopomers (^{25}MgH, ^{26}MgH, ^{25}MgD, and ^{26}MgD) in Table IV, but they can be calculated easily using Eqs. (4) and (5). For example, the explicit form of Eq. (4) for ^{26}MgD is the following:

$$Y^{\mathrm{Mg(26)D}}_{l,m}=\left\{Y^{\mathrm{Mg(24)H}}_{l,m}+\left(\frac{M_{\mathrm{Mg(26)}}-M_{\mathrm{Mg(24)}}}{M_{\mathrm{Mg(26)}}}\right)\delta^{\mathrm{Mg}}_{l,m}+\left(\frac{M_{\mathrm{D}}-M_{\mathrm{H}}}{M_{\mathrm{D}}}\right)\delta^{\mathrm{H}}_{l,m}\right\}\left(\frac{\mu_{\mathrm{Mg(24)H}}}{\mu_{\mathrm{Mg(26)D}}}\right)^{m+l/2}. \quad (6)$$

These constants are available electronically in the EPAPS archive.[32]

Our new equilibrium constants of ^{24}MgH and ^{24}MgD are compared with those previously obtained from the diode laser infrared spectra[27] in Table V. The new ω_e and $\omega_e x_e$ val-

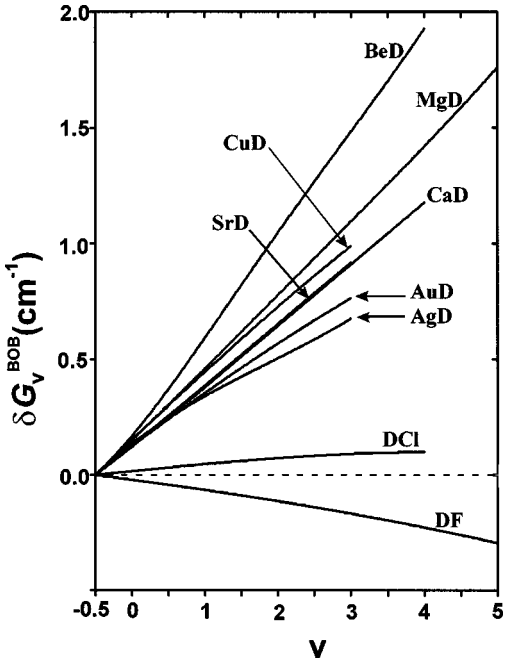

FIG. 5. The contribution of Born–Oppenheimer breakdown correction parameters to the vibrational energies (G_v) of ^{9}BeD, ^{24}MgD, ^{40}CaD, ^{88}SrD, ^{63}CuD, ^{107}AgD, ^{197}AuD, D ^{19}F, and D ^{35}Cl in their ground electronic states, calculated from Eq. (7) and plotted versus the vibrational quantum number of these species. In all cases, the associated fit used the corresponding hydride as the reference isotopomer.

ues are slightly different from the previous ones because only two vibrational intervals were observed in the diode laser infrared spectra. The equilibrium rotational constants ($B_e \approx Y_{0,1}$) of ^{24}MgH and ^{24}MgD have been determined very precisely because we included all pure rotational data in our data set. Using the B_e values of ^{24}MgH and ^{24}MgD, the equilibrium ^{24}Mg–H and ^{24}Mg–D bond distances (r_e) are calculated to be 1.729 721(1) Å and 1.729 157(1) Å, respectively.

DISCUSSION

Several Born–Oppenheimer breakdown correction parameters for the hydrogen atom ($\delta^{\mathrm{H}}_{l,m}$) were required in our combined isotopomer fit. This is not unusual for a diatomic hydride because of its small reduced mass. A total of nine vibrational intervals were observed for the major isotopomers, ^{24}MgH and ^{24}MgD, and we found that nine parameters were required to fit the vibrational energy (G_v) of ^{24}MgH and ^{24}MgD together. Although we have chosen to use five Dunham constants ($Y_{1,0}$ to $Y_{5,0}$) and four Born–Oppenheimer breakdown constants ($\delta^{\mathrm{H}}_{1,0}$ to $\delta^{\mathrm{H}}_{4,0}$) for the vibrational energy, a fit with the same quality was obtained using six vibrational Dunham constants and three Born–Oppenheimer breakdown parameters. The rotational and centrifugal distortion constants required fewer such correction parameters.

In order to illustrate the effect of these correction terms, we calculated the contribution of Born–Oppenheimer breakdown parameters to the vibrational energy of ^{24}MgD using the equation,

$$\delta G_v^{\mathrm{BOB}}(^{24}\mathrm{MgD}) = \sum_l \left\{ Y_{l,0}^{\mathrm{Mg(24)D}} - Y_{l,0}^{\mathrm{Mg(24)H}} \left(\frac{\mu_{\mathrm{Mg(24)H}}}{\mu_{\mathrm{Mg(24)D}}} \right)^{l/2} \right\} \left(v + \frac{1}{2} \right)^l = \sum_l \left\{ \left(\frac{M_{\mathrm{D}} - M_{\mathrm{H}}}{M_{\mathrm{D}}} \right) \delta^{\mathrm{H}}_{l,0} \left(\frac{\mu_{\mathrm{Mg(24)H}}}{\mu_{\mathrm{Mg(24)D}}} \right)^{l/2} \right\} \left(v + \frac{1}{2} \right)^l, \quad (7)$$

where the $\delta^{\mathrm{H}}_{l,0}$ parameters are defined with ^{24}MgH as the reference isotopomer. This correction function is plotted versus the vibrational quantum number (v) of ^{24}MgD in Fig. 5. Similar plots for ^{9}BeD, ^{40}CaD, ^{88}SrD, ^{63}CuD, ^{107}AgD, ^{197}AuD, D ^{19}F, and D ^{35}Cl in their ground electronic states are also presented in Fig. 5, using the Born–Oppenheimer breakdown constants ($\delta^{\mathrm{H}}_{l,0}$) of ^{9}BeH, ^{40}CaH, ^{88}SrH, ^{63}CuH, ^{107}AgH, ^{197}AuH, H ^{19}F, and H ^{35}Cl from literature.[35–39] In all cases, the hydride was the reference isotopomer in the associated fit, and the zeroth order (electronic energy) correction $\delta^{\mathrm{H}}_{0,0}$ is set to zero. The analogous contribution of Born–Oppenheimer breakdown parameters to the rotational constants (B_v) have also been calculated for these molecules using the equation,

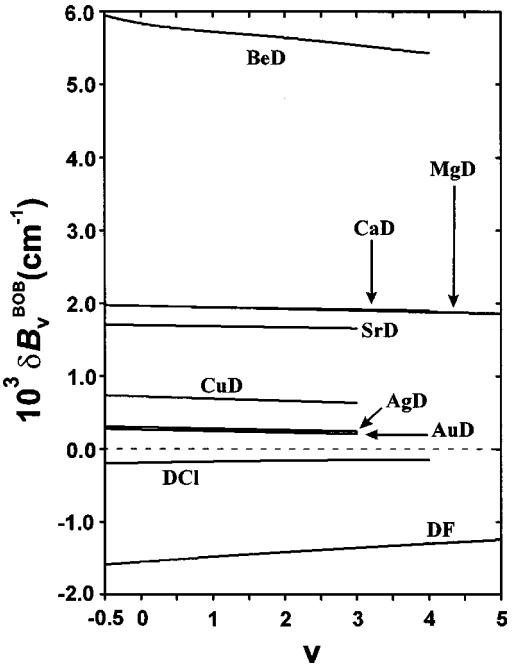

FIG. 6. The contribution of Born–Oppenheimer breakdown correction parameters to the rotational constants (B_v) of ^{9}BeD, ^{24}MgD, ^{40}CaD, ^{88}SrD, ^{63}CuD, ^{107}AgD, ^{197}AuD, D ^{19}F, and D ^{35}Cl in their ground electronic states, calculated from Eq. (8) and plotted versus the vibrational quantum number of these species. In all cases, the associated fit used the corresponding hydride as the reference isotopomer.

$$\delta B_v^{\mathrm{BOB}}(^{24}\mathrm{MgD}) = \sum_l \left\{ Y_{l,1}^{\mathrm{Mg(24)D}} - Y_{l,1}^{\mathrm{Mg(24)H}} \left(\frac{\mu_{\mathrm{Mg(24)H}}}{\mu_{\mathrm{Mg(24)D}}} \right)^{1+l/2} \right\} \left(v + \frac{1}{2} \right)^l = \sum_l \left\{ \left(\frac{M_{\mathrm{D}} - M_{\mathrm{H}}}{M_{\mathrm{D}}} \right) \delta^{\mathrm{H}}_{l,1} \left(\frac{\mu_{\mathrm{Mg(24)H}}}{\mu_{\mathrm{Mg(24)D}}} \right)^{1+l/2} \right\} \left(v + \frac{1}{2} \right)^l, \quad (8)$$

and the associated plots are presented in Fig. 6.

Due to the high quality of the data for all isotopomers, two Born–Oppenheimer breakdown correction parameters for the magnesium atom ($\delta^{\mathrm{Mg}}_{1,0}$ and $\delta^{\mathrm{Mg}}_{0,1}$) have also been determined here. Although the relative magnitudes of $\delta^{\mathrm{Mg}}_{1,0}$ and $\delta^{\mathrm{Mg}}_{0,1}$ are small, their presence implies that the reduced mass ratio relationship is not exactly correct for ω_e and B_e, even for the ^{24}MgH, ^{25}MgH, and ^{26}MgH isotopomers. On the other hand, no correction was required for the spin–rotation interaction constants ($\gamma_{l,m}$), and Eq. (5) was satisfactory.

The MgH/D constants presented in Tables I, II, and IV are suitable for the lower half of the $X\,^2\Sigma^+$ ground state potential well. In future work, we will combine these data with our data from the $A\,^2\Pi - X\,^2\Sigma^+$ and the $B'\,^2\Sigma^+ - X\,^2\Sigma^+$ transitions, which span almost the whole ground state potential well. An analytical potential energy function including the spin-rotation interaction term will be obtained for the $X\,^2\Sigma^+$ ground state of MgH/D by a direct-potential-fit to all experimental data. We expect that an improved value for the dissociation energy of ground state MgH/D will be determined.

CONCLUSION

High resolution Fourier transform infrared emission spectra of MgH and MgD were recorded, and vibration–rotation transitions were observed in the $X\,^2\Sigma^+$ ground electronic state. The new data were combined with existing diode laser infrared[27] and pure rotational data,[24–26,28] and spectroscopic constants were determined for $v=0$ to 4 of ^{24}MgH and $v=0$ to 5 of ^{24}MgD. In a combined fit of the six isotopomers, the Dunham constants and the Born–Oppenheimer breakdown correction parameters were obtained, and the equilibrium ^{24}Mg–H and ^{24}Mg–D bond distances were determined.

ACKNOWLEDGMENTS

We thank C. Demuynck for providing us with some unpublished diode laser infrared and far infrared line positions. Financial support for this work was provided by the Natural Sciences and Engineering Research Council (NSERC) of Canada.

[1] W. W. Watson and P. Rudnick, Astrophys. J. **63**, 20 (1926).
[2] S. Sotirovski, Astron. Astrophys., Suppl. Ser. **6**, 85 (1972).
[3] A. M. Boesgaard, Astrophys. J. **154**, 185 (1968).
[4] E. J. Catanzaro, T. J. Murphy, E. L. Garner, and W. R. Shields, J. Res. Natl. Bur. Stand., Sect. A **70A**, 453 (1966).
[5] P. L. Gay and D. L. Lambert, Astrophys. J. **533**, 260 (2000).
[6] L. Wallace, K. Hinkle, G. Li, and P. F. Bernath, Astrophys. J. **524**, 454 (1999).
[7] P. F. Weck, A. Schweitzer, P. C. Stancil, P. H. Hauschildt, and K. Kirby, Astrophys. J. **582**, 1059 (2003).
[8] P. F. Weck, A. Schweitzer, P. C. Stancil, P. H. Hauschildt, and K. Kirby, Astrophys. J. **584**, 459 (2003).
[9] W. J. Balfour, Astrophys. J. **162**, 1031 (1970).
[10] W. J. Balfour, J. Phys. B **3**, 1749 (1970).
[11] W. J. Balfour and H. M. Cartwright, Chem. Phys. Lett. **32**, 82 (1975).
[12] W. J. Balfour and H. M. Cartwright, Can. J. Phys. **53**, 1447 (1975).
[13] W. J. Balfour and H. M. Cartwright, Can. J. Phys. **54**, 1898 (1976).
[14] W. J. Balfour and H. M. Cartwright, Astron. Astrophys., Suppl. Ser. **26**, 389 (1976).
[15] W. J. Balfour and B. Lindgren, Can. J. Phys. **56**, 767 (1978).
[16] A. C. H. Chan and E. R. Davidson, J. Chem. Phys. **52**, 4108 (1970).
[17] W. Meyer and P. Rosmus, J. Chem. Phys. **63**, 2356 (1975).
[18] M. L. Sink, A. D. Bandrauk, W. H. Henneker, H. Lefebvre-Brion, and G. Raseev, Chem. Phys. Lett. **39**, 505 (1976).
[19] R. P. Saxon, K. Kirby, and B. Liu, J. Chem. Phys. **69**, 5301 (1978).
[20] M. L. Sink and A. D. Bandrauk, Can. J. Phys. **57**, 1178 (1979).
[21] K. Kirby, R. P. Saxon, and B. Liu, Astrophys. J. **231**, 637 (1979).
[22] K. P. Huber and G. Herzberg, *Molecular Spectra and Molecular Structure IV. Constants of Diatomic Molecules* (Van Nostrand, New York, 1979).
[23] P. F. Bernath, J. H. Black, and J. W. Brault, Astrophys. J. **298**, 375 (1985).
[24] K. R. Leopold, L. R. Zink, K. M. Evenson, D. A. Jennings, and M. Mizushima, J. Chem. Phys. **84**, 1935 (1986).
[25] L. R. Zink, Ph.D. thesis, University of Colorado, 1986.
[26] L. R. Zink, D. A. Jennings, K. M. Evenson, and K. R. Leopold, Astrophys. J. Lett. **359**, L65 (1990).
[27] B. Lemoine, C. Demuynck, J. L. Destombes, and P. B. Davies, J. Chem. Phys. **89**, 673 (1988).
[28] L. M. Ziurys, W. L. Barclay, Jr., and M. A. Anderson, Astrophys. J. Lett. **402**, L21 (1993).
[29] A. Shayesteh, D. R. T. Appadoo, I. Gordon, and P. F. Bernath, J. Chem. Phys. **119**, 7785 (2003).
[30] A. Shayesteh, D. R. T. Appadoo, I. Gordon, and P. F. Bernath, Can. J. Chem. (in press).
[31] M. Carleer, Proc. SPIE **4168**, 337 (2001).
[32] See EPAPS Document No. E-JCPSA6-120-001421 for a complete list of all line positions and constants. A direct link to this document may be found in the online article's HTML reference section. The document may also be reached via the EPAPS homepage (http://www.aip.org/pubservs/epaps.html) or from ftp.aip.org in the directory /epaps/. See the EPAPS homepage for more information.
[33] R. J. Le Roy, DPARFIT 3.0, A computer program for fitting multi-isotopomer diatomic molecule spectra, University of Waterloo Chemical Physics Research Report CP-658, 2004. The source code and manual for this program may be obtained from the ''Computer Programs'' link at http://leroy.uwaterloo.ca.
[34] R. J. Le Roy, J. Mol. Spectrosc. **191**, 223 (1998).
[35] R. J. Le Roy, J. Mol. Spectrosc. **194**, 189 (1999).
[36] A. Shayesteh, K. Tereszchuk, P. F. Bernath, and R. Colin, J. Chem. Phys. **118**, 1158 (2003).
[37] A. Shayesteh, K. A. Walker, I. Gordon, D. R. T. Appadoo, and P. F. Bernath, J. Mol. Struct. (in press).
[38] J. Y. Seto, Z. Morbi, F. Charron, S. K. Lee, P. F. Bernath, and R. J. Le Roy, J. Chem. Phys. **110**, 11756 (1999).
[39] T. Parekunnel, T. Hirao, R. J. Le Roy, and P. F. Bernath, J. Mol. Spectrosc. **195**, 185 (1999).